

Purdue University

Purdue e-Pubs

International Compressor Engineering
Conference

School of Mechanical Engineering

2021

Analysis Of Dynamic Heat Transfer Coefficient In a Reciprocating Compressor By Immersed Solid Method in CFD

Rakesh Eettisseri

Tecumseh Products, rakesh.pe@tecumseh.com

Marcelo Real

Sidnei Oliveira

Follow this and additional works at: <https://docs.lib.purdue.edu/icec>

Eettisseri, Rakesh; Real, Marcelo; and Oliveira, Sidnei, "Analysis Of Dynamic Heat Transfer Coefficient In a Reciprocating Compressor By Immersed Solid Method in CFD" (2021). *International Compressor Engineering Conference*. Paper 2653.
<https://docs.lib.purdue.edu/icec/2653>

This document has been made available through Purdue e-Pubs, a service of the Purdue University Libraries. Please contact epubs@purdue.edu for additional information. Complete proceedings may be acquired in print and on CD-ROM directly from the Ray W. Herrick Laboratories at <https://engineering.purdue.edu/Herrick/Events/orderlit.html>

Analysis of Dynamic Heat Transfer Coefficient in a Reciprocating Compressor using the Immersed Solid Method in CFD

Rakesh Eettisseri^{1*}, Marcelo Real², Sidnei Olivera²

¹Tecumseh Products India Pvt Ltd.
Hyderabad, Telangana, India
rakesh.pe@tecumseh.com

²Tecumseh Products Company LLC
5683 Hines Drive, Ann Arbor, MI, USA

*Corresponding autor

ABSTRACT

Accurate mapping of heat transfer inside the Hermetic compressor has been a major challenge for the designing and evaluation of performance. Various methodologies have been adopted for the thermal mapping such as experimental analysis, numerical methods, CFD etc. Mapping is further complex when the motions of multiple components are considered. In this work heat transfer is mapped inside a reciprocating hermetic compressor by considering the rotation of crankshaft and associated motion of connecting rod and piston. The refrigerant gas and oil in the sump are used as the working fluids for this conjugate heat transfer model. The motion is imposed on the moving parts through trigonometric relations using immersed body technique in Ansys CFX. The transient analysis is carried out on a simplified model with few thermally sensitive components to save computation cost. The heat transfer from the omitted components are imposed as boundary conditions in the simplified model. A steady simulation has been done with the simplified model providing 'zero' motion as a reference for comparison and as an initial condition for the transient run. Finally, transient run was carried out and results were compared with the steady state. It has been found that heat transfer between the fluids and components increased up to 600% with the imposed motion. The transient heat transfer coefficients were used in a 1D simulation model and compared with experimental results.

1. INTRODUCTION

Heat transfer inside a hermetic reciprocating compressor is a complex phenomenon. Compressor has two levels of temperatures at inlet and outlet, and heat generation at the motor, heat generation during gas compression process and frictional heat generation at the bearings. Various components are encapsulated inside the housing leading to a complex flow among heat transfer areas, making the accurate thermal mapping tedious. The trade-off between motor cooling by suction gas and resulting increase in suction superheat make the thermal management in compressor design very critical.

Various methodologies have been used for thermal mapping by various researchers around the world in past years. Which involves actual measuring using thermocouples inside the compressor and numerical approaches- like computational fluid dynamics and hybrid methods by combining CFD and 1D heat transfer. Shiva Prasad (1998) and Ribas et al. (2008) have consolidated some of the progressive developments.

An earlier attempt for the actual measurement was done by Meyer and Thompson (1988). Dutra and Deschamps (2010) measured heat flux and validated by energy balancing. Silva et al. (2016) has measured heat flux and temperature using thin film heat flux sensors and thermocouples during ON/OFF cycle operation.

Various researchers considered flow and solid domains of compressors as lumped masses and solved for better understanding of heat and temperature distribution. Meyer and Thompson (1988) developed an analytical heat transfer model in which the energy and mass flow balance equations were solved on the flow area split into various control volumes. Todescat et al. (1992) also adopted similar methods in energy balancing and numerical calculations. Both considered the Heat transfer coefficient through various correlations and experimental data.

Trying to save computational cost from full 3D model, researchers developed hybrid methods. A combination of lumped and 3D methods helped to provide better results by better capturing the heat and temperature distributions at locations where the thermal gradients are higher. Almbauer et al. (2006) developed a thermal network model solving heat transfer equations. He solved the fluid flow in 1D formulation and the conductive heat transfer in 3D formulation. Sanvezzo and Deschamps (2012) also considered a hybrid model in which the conduction heat transfer was solved in 3D and the convection in lumped modelling approach. Posch et al. (2016) worked on CFD model for suction and discharge gases and 3D numerical on solid part but lumped analysis for gas in shell and lubrication oil.

3D numerical analysis became the favorite among researchers because of its accuracy, despite its high computational cost. Sivaprasad (2004) discussed about the needs, benefits and risks of using CFD approach for positive displacement compressors. He concluded by reminding the users that CFD is not a magic wand and it has to be trusted only after verification and validation. Numerical 3D simulations focused on certain areas of interests such as suction superheat done by Lacerda and Takemori (2014). Chikurude et al. (2002) and Birari et al. (2006) modelled the entire compressor with conductive and convective heat transfer through CFD approach. Raja (2003) had also modelled the full compressor considering oil at the bottom. Lacerda and Takemori (2016) also performed a detailed simulation by discretizing solid and fluid components as 3D with motor and frictional heat generation.

In this work a full transient CFD model of a compressor is developed regarding crankshaft, connecting rod and piston as moving parts, which induced motion to the oil/gas inside the shell. The simulation was performed in Ansys CFX, where the crankshaft and connecting rod were assumed as immersed bodies and piston motion has been captured through moving mesh as it moves linearly whereas the motion of other two moving components are non-linear and unsymmetrical. For this evaluation it was considered R404A refrigerant gas and POE 32 oil. In order to reduce computational cost in transient simulation, we only considered the domains, which are highly influenced by the oil dynamics and heat transfer from other components were imposed as boundary conditions which are obtained through a complete steady model. A few iterations with 'zero' motion run was carried out and used to initiate the transient run before imposing motion. The compressor had to run for a few cycles to understand the dynamics of heat transfer characteristics. Due to the thermal inertia of components, achieving steady temperatures of components must bear high computational cost. So, a 1D model of compressor with all the components was simulated in GT-Suite platform, using the heat transfer coefficients from CFD. The results were compared with experimental results and the variations are lying under 10%.

2. METHODOLOGY

2.1 Motion Equations

In the model, motion was imposed to 3 components: crankshaft, piston and connecting rod. Crankshaft in rotational motion, piston in linear motion and connecting rod in semi-circular motion at an angular velocity about the smaller end, which also moves with piston. The model is developed based on the work of Nigus (2016).

From the Figure 1, the angular velocity of the crankshaft is,

$$\omega = \frac{d\theta}{dt} \quad (1)$$

The displacement of piston from TDC,

$$x = l(1 - \cos \phi) + r(1 - \cos \theta) \quad (2)$$

From the figure, the value of $\cos \phi$ can be obtained after factorising and neglecting higher powers of λ ,

$$\cos \phi = 1 - \frac{(\lambda \sin \theta)^2}{2} \quad (3)$$

The angular velocity of connecting rod about small end,

$$v = \frac{d\phi}{dt} = \lambda \omega \cos \theta \quad (4)$$

Equations (1), (2) and (4) defines the motion equations of crankshaft, piston and connecting rod respectively with known values.

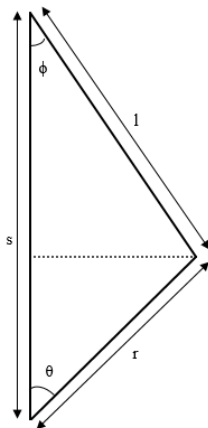


Figure 1: schematic of crank mechanism

2.2 Simulation Methodology

The motion is imposed over crankshaft and connecting rod which are assumed as solids immersed in a fluid medium representing its shape, orientation, position and velocity (Ansys CFX theory guide). The solver imposes a source of momentum to the fluid overlapped by the solid domain at its boundary. In effect, the fluid surrounding the body will behave as if it is flowing around it, although the immersed bodies cannot take the heat transfer. Therefore, in this method, the heat transfer from/to these moving bodies are neglected. As the piston is moving linearly, hexagonal moving meshes can be used to represent the piston motion without much complexity unlike other unsymmetrical, nonlinear moving bodies.

The oil-refrigerant flow field is solved as a Homogeneous multiphase flow. In this Eulerian- Eulerian model, both the fluids share the same flow fields. With free surface flow interface, the flow domain will have a clear and distinguishable interface. Buoyancy is activated to capture the density induced flow and heat transfer. The simulation is solved with forward upwind method with SST turbulent model. The total number of elements including the boundary layers is 5.8 million.

Crankshaft and connecting rod are used as the immersed bodies and will impose momentum into the flow field. Even though the motion of piston is imposed through moving mesh, piston was also considered as an immersed body for better visualisation in post processing. Initially it is solved the entire flow field with oil sump, cavity gas, discharge gas and suction gas with all the solid components in CFD for steady Heat Transfer Coefficient. Oil lubrication circuit is not considered. Heat transfer inside the cylinder is also not considered. Instead, a flow outlet from suction side and flow inlet to discharge side was given with appropriate conditions. The domains which are not highly influenced by oil dynamics are disabled in the transient run and heat transfer from these domains would serve as boundary conditions. The simplified model was run for few iterations with no motion imposed, to initiate the transient run. Then the transient run was started with the motion equations above defined on respective components.

Some minor components like brackets, mounting springs etc. are not considered for the simulation. The full geometry is simplified at the blends and small gaps to reduce the number of meshes. Airgaps, gaskets, insulators etc. are replaced with corresponding thermal contact resistance values before the simulation. Heat generated by the motor is also added as volumetric heat generation in the motor parts. Cross sectional views of the model considered for full steady and transient simulations are shown in Figure 2.

The compressor simulation was run at 60Hz and ASHRAE LBP condition: -23.3°C evaporator temperature, 54.4°C condenser temperature and 32.2°C return gas temperature. Mass flow, discharge temperature for R404A were imposed accordingly. The ambient temperature was at 32.2°C and ambient-housing heat transfer coefficient was kept at 40

W/m²K as the compressor was exposed to an air flow in the calorimeter setup. The matrix of Interfaces and boundary conditions for the transient is marked in Table 1 like Lacerda and Takemori (2016) with domain description in the first column and row. In the matrix, the heat transfer from/to the disabled domains are marked as boundary conditions and no connection assigned from/to the immersed body as it cannot take any heat transfer. A cross sectional view of flow domains in full model and transient model are shown in Figure 2. The steady model was meshed with 8.1 million elements which is taking 45 hours for 1500 iteration for a 32Gb 4 core simulation. For transient run with 5.8 million elements is taking 17 hours to complete one cycle with 2degree steps for same configuration with 12 cores. The average courant number for transient simulation is under 10.

Table 1: Matrix of heat transfer interface and boundaries between parts for transient run

	C G	S O	S G	D G	S T	H S	S M	C H	V P	C C	D M	S L	D T	S R	R O	W D	C S	C R	P N	
CG	Enabled domain	Interface	Interface																	
SO	Interface	Enabled domain	Interface	Interface																
SG	Interface	Interface	Enabled domain	Interface	Interface															
DG	Interface	Interface	Interface	Enabled domain	Interface	Interface														
ST	Interface	Interface	Interface	Interface	Enabled domain	Interface	Interface													
HS	Interface	Interface	Interface	Interface	Interface	Enabled domain	Interface	Interface												
SM	Interface	Interface	Interface	Interface	Interface	Interface	Enabled domain	Interface	Interface											
CH	Interface	Enabled domain	Interface	Interface																
VP	Interface	Enabled domain	Interface	Interface																
CC	Interface	Enabled domain	Interface	Interface																
DM	Interface	Enabled domain	Interface	Interface																
SL	Interface	Enabled domain	Interface	Interface																
DT	Interface	Enabled domain	Interface	Interface	Interface	Interface	Interface	Interface	Interface											
SR	Interface	Enabled domain	Interface	Interface	Interface	Interface	Interface	Interface												
RO	Interface	Enabled domain	Interface	Interface	Interface	Interface	Interface													
WD	Interface	Enabled domain	Interface	Interface	Interface	Interface														
CS	Interface	Enabled domain	Interface	Interface	Interface															
CR	Interface	Enabled domain	Interface	Interface																
PN	Interface	Enabled domain	Interface																	

 Enabled domain
 Disabled domain
 Boundary condition

 immersed body
 no connection assigned

Because of the thermal inertia of bulky compressor components, it will be computationally very costly to achieve a repeatable transient heat transfer at each cycle. So, a few cycles only simulated to understand the variation of heat transfer and the maximum percentage of variation of heat transfer from previous cycle of any heat transfer coefficient

was reduced to 5% at 15th cycle. A 1D model also created in GT-Suite with the same full geometry and boundary conditions and average of transient Heat transfer coefficients from steady and transient CFD cases are imposed on the interfaces. The final temperatures from 1D models and experimental results are compared and found within the range of 10%.

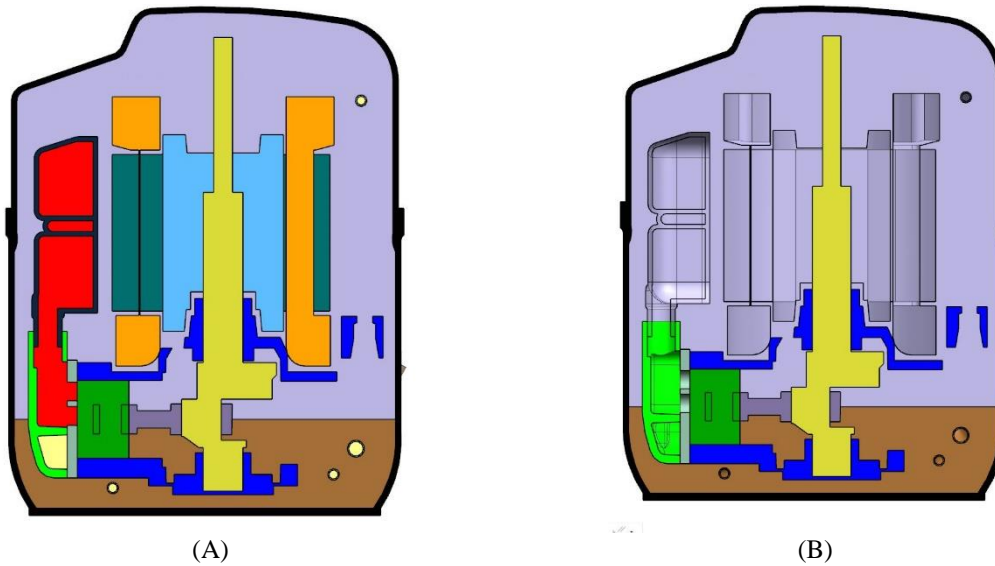


Figure 2: Cross sectional front view of domains on (A) steady full model and (B) Transient model

2.3 Experimental Setup

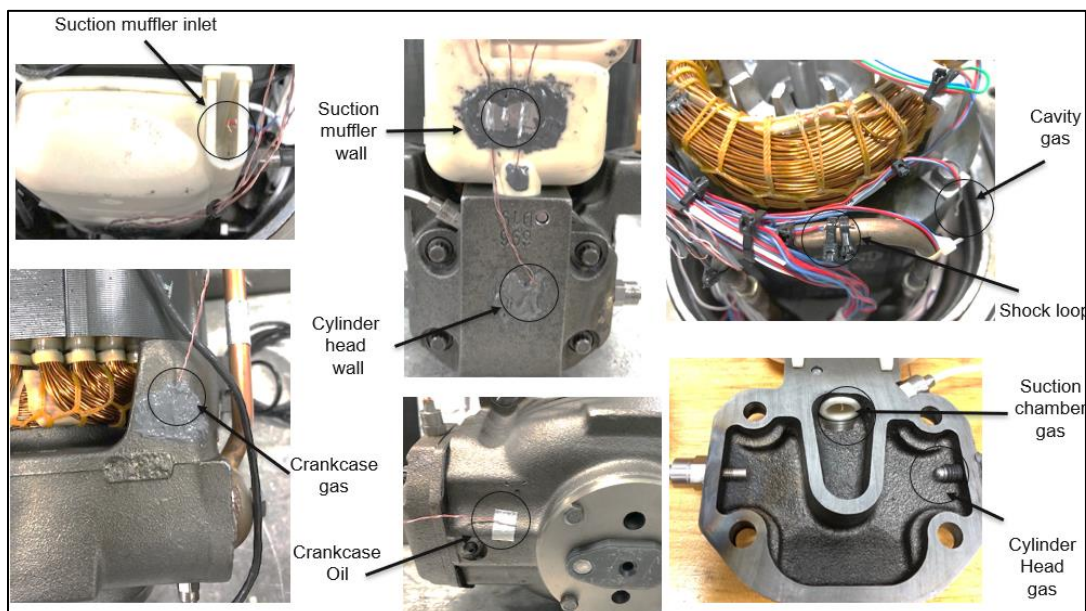


Figure 3: Thermocouples position - Compressor kit

T-type Thermocouples were installed to measure the compressor temperatures at different positions: suction muffler inlet, suction muffler wall, suction chamber, cylinder head gas, cylinder head wall, shock loop, crankcase (oil side and gas side), cavity gas, oil sump, suction and discharge tube and also upper and lower housing. The T-type

thermocouples range are from -200°C to 350°C and have the accuracy of $\pm 1\text{C}$ or $\pm 0.75\%$. National Instruments CDAQ NI9178 chassis, NI9212 temperature module and software LabView were used to acquire the data. The location of thermocouples installed are in the Figure 3.

3. RESULTS AND DISCUSSION

A Cross sectional view of the compressor with gas and oil domains at the beginning of the transient or steady case and at the end of the 15th cycle is shown in Figure 4. Some oil waves can be observed due to the moving components into the fluids. These movements increase the heat transfer inside the gas/oil domains. Figure 5 shows the volume fraction of oil at different positions of crank rotations during different cycles. The waves will spread inside the compressor after few cycles and the wave fronts may bounce back from the surfaces, which also may generate secondary, tertiary wave fronts. The simulation will be computationally very costly to track all the waves generated. So, the simulation is stopped at 15 cycles (0.3 sec) when the magnitude of average heat flux difference through various interfaces are near or less than 5% of the previous cycle.

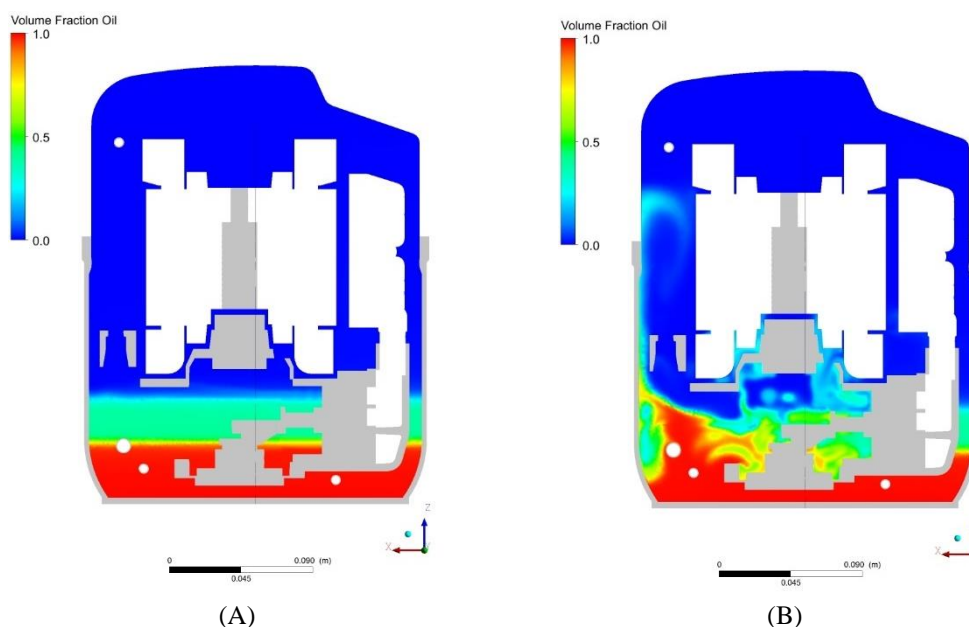


Figure 4: Cross sectional front view of fluid domains at (A) steady and (B) at the end of 15 cycles

The average heat transfer over a cycle from the beginning to the 15th cycle is plotted in Figure 6. The development of heat transfer over cycles are in good agreement with the shape of flow domains. The crankcase has a shape which bounds the fluid from all direction except one which is opposite to the piston side. As a result, the sudden increase in the heat transfer of crankcase gas/oil interfaces are very evident. Shock loops and discharge mufflers are lying opposite to the piston where the velocity is high, consequently the heat transfer is also very high. The cylinder head and valve plate are the farthest from the sources of motion. As the waves had to travel around the crankcase, the heat transfer is increased very slowly and lightly.

The variation of the heat transfer coefficients over a cycle at the 15th cycle for different interfaces are in Figure 7. After a few cycles a periodic pattern of heat flux started to appear showing some variations in the magnitude, however the temperature changes happen at a very slow rate due to the thermal inertia. Till the end of last cycle maximum increase in any component was less than 0.3% except cavity which is 1.75% higher. It is evident due to the mixing of oil in the gas domain.

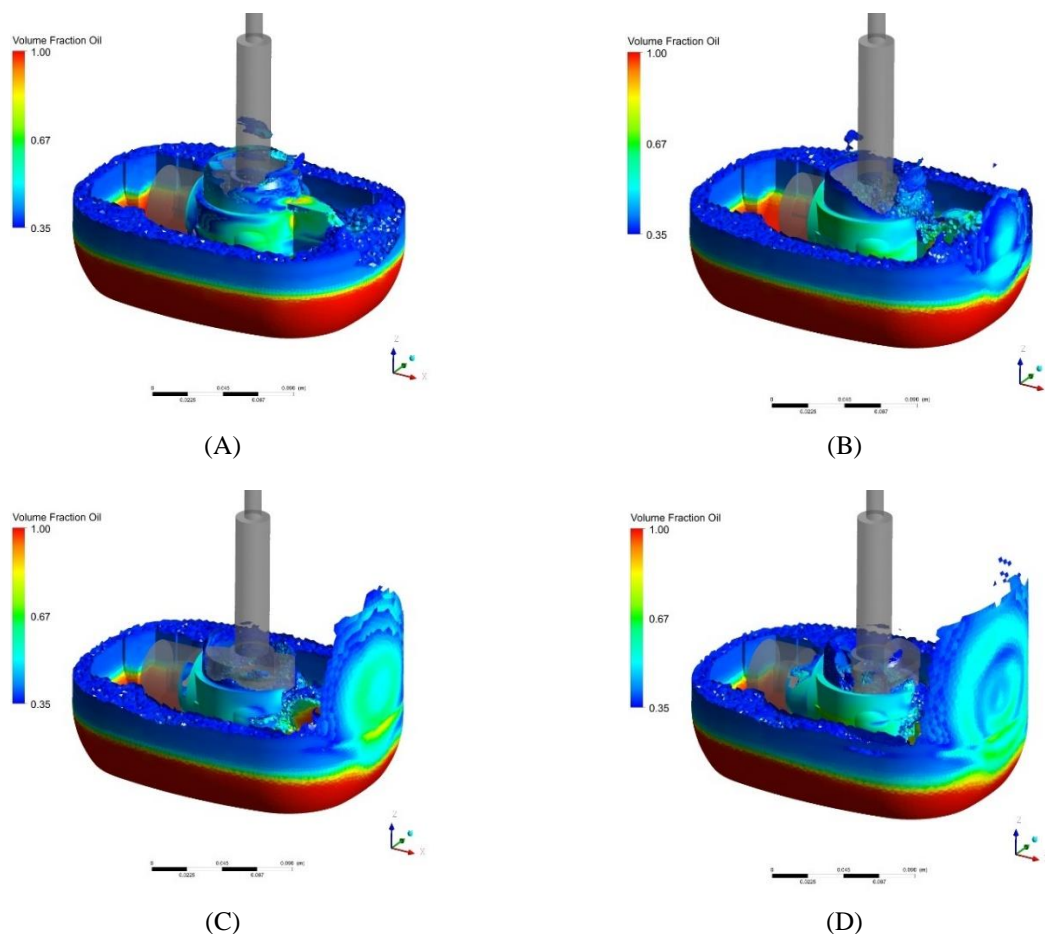


Figure 5: Oil volume fraction at (A) 270° of 3rd cycle (B) 180° of 7th cycle (C) 90° of 11th cycle and (D) end of 15th cycle

of oil in the gas domain. Change in sump domain is only 0.28%. The contact area between oil/gas interfaces with other components also will change, but as the calculation was based on dimensions fixed in CFX domains, contact area was also considered as constant. The average Heat Transfer Coefficient was calculated from the equation 5. The average heat transfer coefficient over the last cycle is calculated and compared with steady heat transfer coefficient in Table 2.

$$Q = hA\Delta T \quad (5)$$

Two 1D simulations were done, one with steady and other updated with transient heat transfer coefficients. In the transient model, whichever coefficients are not calculated by transient CFD were kept as it is in steady. GT-Suite can calculate the average temperature as well as the temperature at the interface called as port temperature. As per the thermocouple locations in actual test, for large components like crankcase and housing port locations were considered for comparison and for other components average temperatures were compared. The results are plotted in Figure 8.

Immersed bodies can be assumed as virtual bodies which can only transfer momentum to the fluid it surrounds through its boundaries but it itself replaced by the fluid in which it is immersed. So, this body cannot take part in the heat transfer process which can contribute deviations in the actual prediction of heat transfer. Also, the presence of additional fluid which replace the immersed bodies can also contribute. Introducing moving mesh can eliminate these chances of errors. But the asymmetric shape and non-linear motion of moving components will make the meshing a hectic task. But the flow dynamics and heat transfer behaviour were captured through this method for initial few cycles. Simulation with a greater number of cycles can be performed with high computational cost.

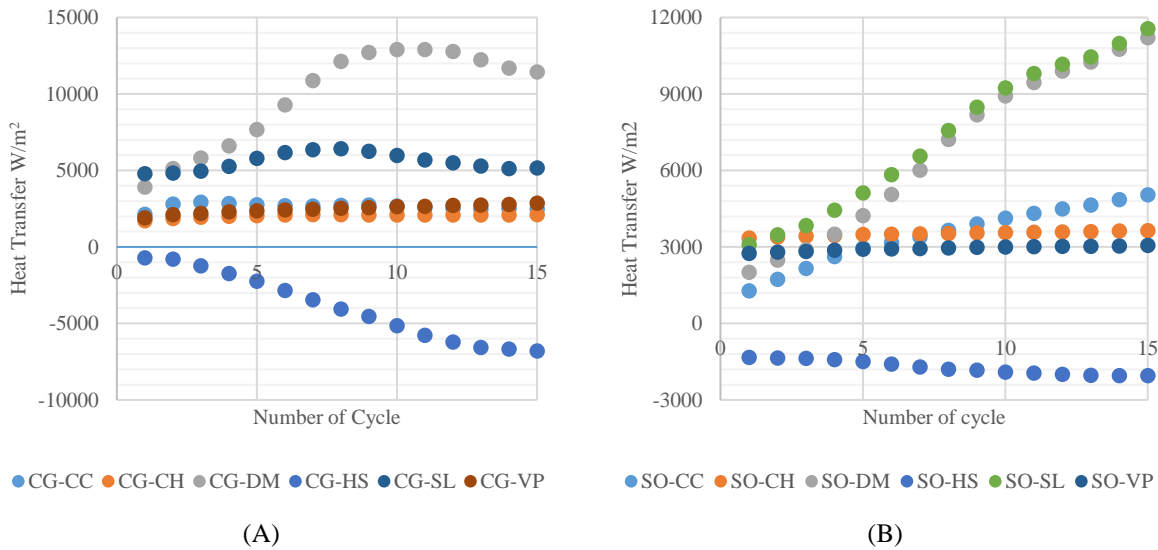


Figure 6: Cycle Averaged Heat transfer of various interfaces with (A) Cavity domain and (B) sump domain

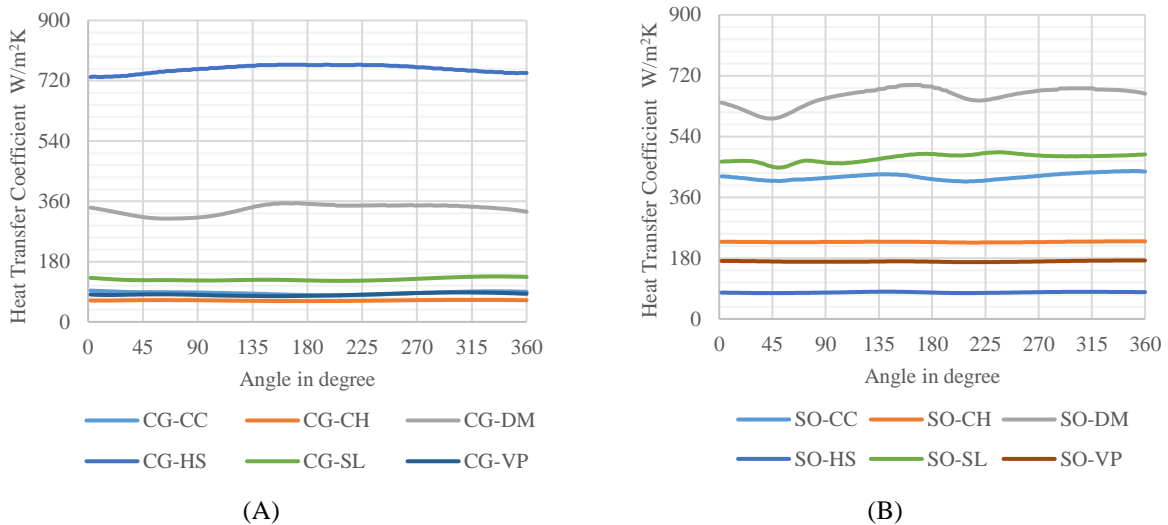


Figure 7: Variation of Heat Transfer Coefficients in a cycle of various interfaces with (A) Cavity domain and (B) Sump domain

4. CONCLUSION

In this work, a CFD approach was used to estimate the transient heat transfer coefficients inside the compressor and used them on a 1D simulation model, having the model validated by experimental results. Moving components were considered as immersed bodies with induced motion into the fluid domain of refrigerant gas and oil in the sump. A comparison of steady and transient heat transfer coefficients was done and applied on a 1D model to obtain the simulated results. The computational time of transient solution is high compared to steady analysis. To save computational time, only few key components were considered in transient CFD simulation. At some interfaces, heat transfer coefficient increased up to 6 times with transient analysis. The final output temperatures from the 1D were compared with experimental results and it was found a difference under 10%. The Immersed body in Ansys CFX can only transfer momentum through its boundaries without replacing any fluid or taking up heat. To save computational time simulation was continued only for 15 cycles and transient simulation was limited to just a few components. These might be some reason for the variation. By considering the immersed bodies as regular solid

bodies, the flow domain as moving meshes and by considering all the components into picture, a better prediction can be performed but at the cost of huge computational time.

Table 2: Steady heat transfer coefficient

	CG						SO					
W/m^2K	CC	CH	DM	HS	SL	VP	CC	CH	DM	HS	SL	VP
Steady	34.9	40.6	75.8	162.8	100.9	42.3	85.5	218.6	94.9	46.4	122.6	170.0
Transient	86.2	63.9	336.7	754.4	125.4	82.0	420.8	228.0	659.4	78.7	476.6	170.1
change	147.3%	57.1%	344.4%	363.6%	24.3%	93.6%	392.3%	4.3%	594.7%	69.3%	288.8%	0.1%

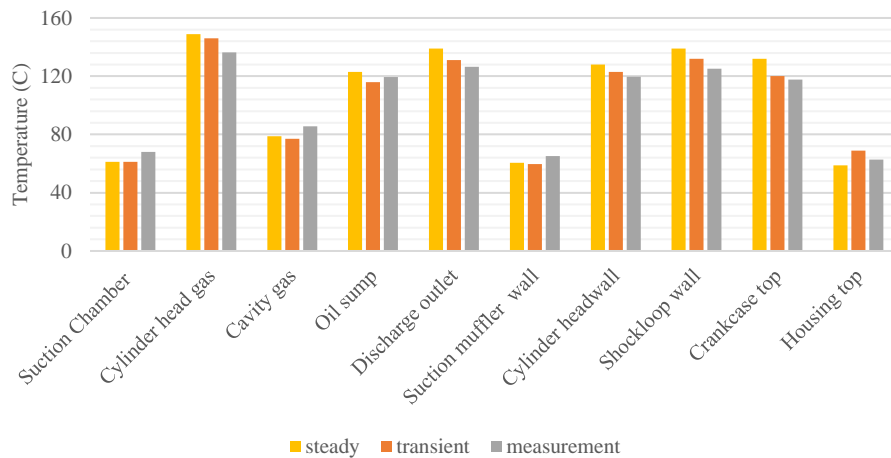


Figure 8: Comparison chart of temperature from 1D simulation

NOMENCLATURE

CG	Cavity gas	DT	Discharge tube
SO	Sump oil	SR	Stator
SG	Suction gas	RO	Rotor
DG	Discharge gas	WD	Winding
ST	Suction tube	CS	Crank shaft
HS	Housing	CR	Connecting rod
SM	Suction muffler	PN	Piston
CH	Cylinder head	l	Length of connecting rod
VP	Valve plate	r	Radius of throw
CC	Crankcase	θ	Crank angle
DM	Discharge mufflers	ϕ	Angle of rotation of conrod
SL	Shock loops	λ	r/l

REFERENCES

Ansys CFX theory guide, 2018

Almbauer, R., Burgstaller, A., Abidin Z. & Nagy D. (2006), *3-Dimensional Simulation for Obtaining the Heat Transfer Correlations of a Thermal Network Calculation for a Hermetic Reciprocating Compressor*, Proc. Int. Compressor Eng. Conf. Purdue, paper 1794

- Birari, Y. V., Gosavi, S.S & Jorwekar, P. P. (2006), *Use of CFD in Design and Development of R404A Reciprocating Compressor*, Proc. Int. Compressor Eng. Conf. Purdue, paper 1727
- Chikurude, R.C., Longanathan, E., Dandekar, D. P. & Manivasagam, S. (2002), *Thermal Mapping of Hermetically Sealed Compressors Using Computational Fluid Dynamics Technique*, Proc. Int. Compressor Eng. Conf. Purdue, paper 1520
- Dutra, T. & Deschamps, C. J. (2010), *Experimental Investigation of Heat Transfer in Components of a Hermetic Reciprocating Compressor*, Proc. Int. Compressor Eng. Conf. Purdue, paper 2002
- Lacerda, J. F. & Takemori, C. K. (2014), *Predicting the Suction Gas Superheating in Reciprocating Compressors*, Proc. Int. Compressor Eng. Conf. Purdue, paper 2332
- Lacerda, J. F. & Takemori, C. K. (2016), *CFD Approach to Evaluate Heat Transfer in Reciprocating Compressors*, Proc. Int. Compressor Eng. Conf. Purdue, paper 2487
- Meyer, W. A. & Thompson, H. D. (1988), *An Experimental Investigation into Heat Transfer to the Suction Gas in a Low-Side Hermetic Refrigeration Compressor*, Proc. Int. Compressor Eng. Conf. Purdue, paper 661
- Meyer, W. A. & Thompson, H. D. (1988), *An Analytical Model of Heat Transfer to the Suction Gas in a Low-Side Hermetic Refrigeration Compressor*, Proc. Int. Compressor Eng. Conf. Purdue, paper 662
- Nigus H., 2015, *Kinematics and Load Formulation of Engine Crank Mechanism*, *Engineering Journal*, Magnolithe, 10.13140/RG.2.1.3257.1928
- Posch, S., Hopfgartner, J., Heimel, M., Berger E. & Almbauer R. (2016), *Thermal Analysis of a Hermetic Reciprocating Compressor Using Numerical Methods*, Proc. Int. Compressor Eng. Conf. Purdue, paper 2429
- Raja, B., Sekhar, S. J., Lal D. M. & Kalanidhi, A. (2003), *A numerical Model for Thermal Mapping in a Hermetically Sealed Reciprocating Refrigerant Compressor*, *International Journal of Refrigeration* 26 (2003) 652–658
- Ribas Jr., F. A., Deschamps, C. J., Fagotti, F., Morriesen, A., & Dutra, T. (2008), *Thermal Analysis in Reciprocating Compressors – A Critical Review*, Proc. Int. Compressor Eng. Conf. Purdue, paper 1907
- Sanvezzo Jr., J. & Deschamps, C.J. (2012), *A Heat Transfer Model Combining Differential and Integral Formulations for Thermal Analysis of Reciprocating Compressors*, Proc. Int. Compressor Eng. Conf. Purdue, paper 2210
- Shiva Prasad, B.G. (1998), *Heat Transfer in Reciprocating Compressors - A Review*, Proc. Int. Compressor Eng. Conf. Purdue., paper 1349
- Shiva Prasad, B.G. (2004), *CFD for Positive Displacement Compressors*, Proc. Int. Compressor Eng. Conf. Purdue, paper 1689
- Silva, L.M., Dutra, T. & Deschamps, C. J. (2016), *Experimental Investigation of Heat Transfer in Components of a Hermetic Reciprocating Compressor under Thermal Transient*, Proc. Int. Compressor Eng. Conf. Purdue, paper 2464
- Todescat, M. L., Fagotti, F., Prata., A. T. & Ferreira, R. T. S. (1992), *Thermal Energy Analysis in Reciprocating Hermetic Compressor*, Proc. Int. Compressor Eng. Conf. Purdue, paper 936

ACKNOWLEDGEMENT

To Tecumseh Products Company LLC and Tecumseh Products India Pvt Ltd. for the financial support.